

Influence of Chemisorption on the Thermal Conductivity of Single-Wall Carbon Nanotubes

Clifford W. Padgett* and Donald W. Brenner

Department of Materials Science and Engineering, North Carolina State University,
Raleigh, North Carolina 27695

Received March 4, 2004; Revised Manuscript Received April 20, 2004

ABSTRACT

The thermal conductivity at 300 K of (10,10) carbon nanotubes that have been functionalized by chemical attachment of phenyl rings through covalent bonding (chemisorption) at random positions has been calculated as a function of adsorption density using classical trajectories. The system exhibits a rapid drop in thermal conductivity with chemisorption, where chemisorption to as little as 1.0% of the nanotube carbon atoms reduces the thermal conductivity by over a factor of 3. The simulation results indicate that the effect is due to a reduction in phonon scattering length rather than changes in the vibrational frequencies of the carbon atoms in the nanotube.

Thermal conductivities of 300–6600 W/m-K in the axial direction of isolated (10,10) carbon nanotubes (CNTs) calculated from molecular simulations^{1–4} together with experimental measurements of 1750–5850 W/mK for CNT mats^{5–7} suggest that CNTs may have applications for thermal management in polymer composites. However, direct experimental measurements of the thermal properties of CNT–polymer composites show mixed results; some groups report that the addition of a small percentage of carbon nanotubes to a polymer matrix greatly improves the system's thermal conductivity,^{8,9} while others report that the effect is less than predicted and is controlled by the interface thermal conductance.¹⁰ One possible way to improve the thermal conductance between CNTs and a support matrix is by chemically functionalizing the CNT into the matrix. Modeling studies have suggested that such functionalization can improve load transfer in CNT–polymer composites without significantly sacrificing the high axial Young's modulus of CNTs.^{11,12} While the thermal conductivity of CNTs with topological defects has been calculated,³ studies involving the influence of chemical functionalization on thermal properties of CNTs have not been reported.

In the following, we report thermal conductivities of isolated (10,10) CNTs on which phenyl groups have been attached that are calculated using classical trajectories. Our simulations predict that thermal conductivities for pristine CNTs are greater than ~350 W/mK and require lengths exceeding ~0.15 μm to obtain values that are independent of length, in agreement with prior modeling studies. In contrast, we show that chemisorbing phenyl groups to as

little as 1.0% of the carbon atoms in a CNT reduces the predicted thermal conductivity by greater than a factor of 3, and reduces the nanotube length needed for the calculated thermal conductivity to converge to about 15 nm, or 16 times the average distance along the tube axis between chemisorbed species. The phonon power spectrum for carbon atoms in the CNTs at 300 K, which was also obtained from classical trajectories, shows a slight broadening of the highest frequency optic mode due to chemisorption with little change to the acoustic modes. These results, together with the convergence of thermal conductivity with nanotube length, suggest that the reduction in thermal conductivity due to chemisorption comes from a reduction in phonon scattering length and not from shifts in the vibrational frequencies.

The thermal conductivities of the CNTs were calculated using a straightforward method introduced by Müller-Plathe in which a cold and a hot region of the system are created by switching the velocity of the hottest atom in the cold region with the velocity of the coldest atom in the hot region.¹³ This results in a known quantity of heat flux J transferred between the regions of

$$J = \frac{\sum_{i=1}^n \frac{1}{2} m_i (v_{h_i}^2 - v_{c_i}^2)}{2At} \quad (1)$$

where m is the mass of the atoms, t is the time in the simulation, A is the cross sectional area, v_h and v_c are the velocities chosen from the cold and hot regions, respectively, and n denotes the number of transfers. After the system reaches equilibrium (i.e., the heat transferred along the

* Corresponding author. E-mail: cliffop@alumni.clemson.edu; Phone: 919-513-2424; Fax 919-515-7724.

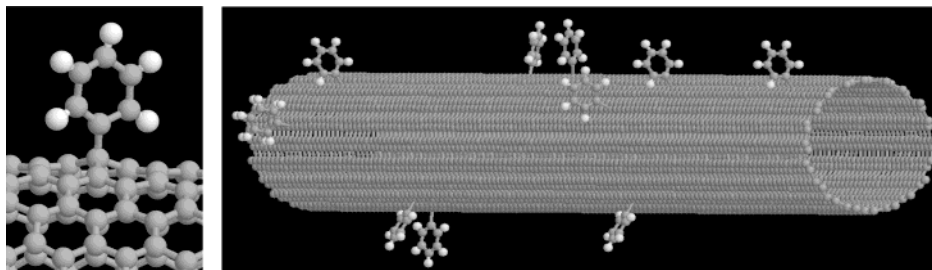


Figure 1. Illustrations of a (10,10) nanotube with phenyl groups randomly chemisorbed to 1.0% of the carbon atoms.

nanotube between the two regions equals the heat transfer created by the velocity switching), the thermal conductivity λ is obtained as

$$\lambda = - \frac{\langle J(t) \rangle}{\langle \partial T / \partial z \rangle} \quad (2)$$

where dT/dz is the temperature gradient along the CNT axis and the brackets denote a statistical time average. Equation 2 is formally correct in the limit that the temperature gradient approaches zero and in the limit that time approaches infinity. For practical applications, however, the ratio in eq 2 produces a reasonable value provided that the system is fully equilibrated and the simulation is sampled over a sufficiently long time.

A many-body bond order function was used to describe the interatomic forces.¹⁴ This potential function, which has been used widely for hydrocarbon systems,¹² analytically describes energies and force for both sp^2 and sp^3 bonding, depending on local coordination and the degree of conjugation. Classical equations of motion for each atom were numerically integrated using a third-order Nordsieck predictor-corrector algorithm and a time step size 0.25 fs. A periodic boundary condition was applied along the tube axis, and the length of the supercell was varied to explore the dependence of thermal conductivity on CNT length. Chemically functionalized CNTs were made by attaching phenyl groups to the nanotube carbon atoms and allowing the system to equilibrate at 300 K for 2.5 ps before beginning thermal conductivity runs. The thermal conductivity was calculated using the method described above, with the velocity being exchanged between hot and cold regions, each of which was 20 atoms in size (one unit cell), every 15 fs. The thermal exchange ran for at least 100 ps or until steady-state was achieved (signified by convergence of thermal conductivity with respect to time). Data were sampled and averaged over every 2.5 ps time period to obtain the thermal gradients. The cross-sectional area used for the flux was an annular ring 3.4 Å thick.

The phonon power spectrum $D(\omega)$ at 300 K was calculated from the atomic velocities extracted every 10 time steps (2.5 fs) for 615 Å long CNTs at each degree of functionalization using the equation

$$D_\alpha(\omega) = \frac{1}{4\pi T} \langle |\int_0^{2T} v_\alpha(t) e^{-i\omega t} dt|^2 \rangle \quad (3)$$

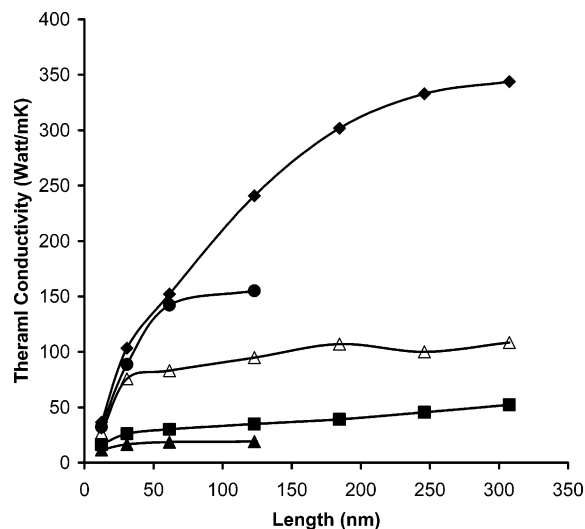


Figure 2. Thermal conductivity versus nanotube length for various degrees of functionalization. Diamonds 0%, circles 0.25%, open triangles 1%, squares 5%, and triangles 10% functionalized.

Here $v_\alpha(t)$ is the atomic velocity in cylindrical coordinates r , θ , and z , $2T$ is the simulation time, and the brackets denote a statistical time average over all of the atoms in the CNTs. In general, eq 3 converges faster and produces a smoother spectrum than Fourier transforming the velocity autocorrelation function.¹⁵

Simulations were performed on pristine CNTs and CNTs on which 0.25%, 1%, 5%, or 10% of the carbon atoms had a bonded phenyl group. The case where phenyl groups are attached to 1% of the atoms on a nanotube is illustrated in the left panel of Figure 1. The atoms on which the phenyl groups are bonded have hybridizations that change from sp^2 to sp^3 . The associated change in geometry of these atoms is illustrated in the right panel of Figure 1, where the bonded nanotube atoms are “raised” away from the nanotube axes. The remaining atoms, including those in the phenyl group, remain sp^2 bonded. The bond order potential predicts a binding energy of 3.03 eV with respect to a pristine nanotube and an isolated phenyl group, a value that is characteristic of reasonably strong covalent bonding.

Plotted in Figure 2 as the solid diamonds is the calculated thermal conductivity for a pristine (10,10) CNT as a function of the length of the periodic supercell used in the simulations. The thermal conductivity value increases with increasing CNT length up to a length of at least $\sim 0.15 \mu\text{m}$, where a thermal conductivity of 350 W/mK is calculated (this value represents both length convergence and thermal gradient

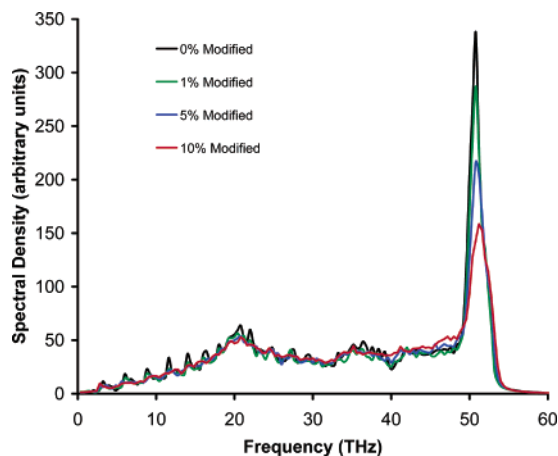


Figure 3. Phonon spectra for carbon nanotubes 615 Å long with various degrees of functionalization.

convergence since flux is constant). This value is therefore a lower limit on the thermal conductivity for an isolated (10,10) CNT. This result suggests that the phonon scattering length is longer than about $0.15\ \mu\text{m}$, consistent with prior simulations. Also plotted in Figure 2 is the thermal conductivity for the four degrees of functionalization studied. The functionalized CNTs all show significantly smaller thermal conductivities that converge well with respect to periodic cell length for cells greater than about 615 Å. The faster convergence implies a much shorter scattering length for phonons in the functionalized CNT compared to those in the pristine structure. The simulations predict a decrease in thermal conductivity of at least a factor of 3 with as little as 1.0% of the atoms in the CNT being functionalized. Functionalization of 5% and 10% continues to degrade the thermal conductivity, but to a much lesser degree compared to the drop from a pristine to 1.0% functionalization.

Plotted in Figure 3 is the phonon power spectrum for carbon atoms in the pristine CNT and in the CNTs with the three degrees of functionalization studied. There is a slight broadening of the highest frequency carbon–carbon optical mode with increasing functionalization. This broadening likely arises from an increase in the number of sp^3 bonded carbon atoms in the nanotube. Also, the introduction of sp^3 carbons into the nanotube structure creates defects for the phonons to interact with and scatter off of, thus reducing the mean free path of the phonons. The low frequency

acoustic modes, however, are almost identical for each type of nanotube. This result, together with the convergence properties of the thermal conductivity with respect to cell size, suggests that the degradation of thermal conductivity with functionalization arises almost entirely from a reduction in the scattering length rather than specific changes in the vibrational modes arising from functionalization.

We have reported here the thermal conductivities of single-walled (10,10) CNTs on which phenyl groups have been chemically attached calculated using molecular dynamics simulations. The results show that functionalization of nanotubes at densities as low as 1.0% of functionalized carbon atoms drastically reduces their thermal conductivity. This indicates that increasing the heat transfer between CNTs and a polymer matrix in a composite via chemical cross-linking may be counterproductive as it would severely compromise the thermal properties of the CNT.

Acknowledgment. This work was supported by NASA (NAG-1-01061).

References

- (1) Osman, M. A.; Srivastava, D. *Nanotechnol.* **2001**, *12*, 21–24.
- (2) Berber, S.; Kwon, Y. K.; Tománek, D. *Phys. Rev. Lett.* **2000**, *84*, 4613–4616.
- (3) Che, J.; Çagin, T.; Goddard, W. A., III *Nanotechnol.* **2000**, *11*, 65–69.
- (4) Maruyama, S. *Physica B* **2002**, *323*, 193–195.
- (5) Hone, J.; Whitney, M.; Piskoti, C.; Zettl, A. *Phys. Rev. B* **1999**, *59*, R2514–R2516.
- (6) Yi, W.; Lu, L.; Zhang, D.-L.; Pan, Z. W.; Xie, S. S. *Phys. Rev. B* **1999**, *59*, R9015–R9018.
- (7) Hone, J.; Llaguno, M. C.; Nemes, N. M.; Johnson, A. T.; Fisher, J. E.; Walters, D. A.; Casavant, M. J.; Schmidt, J.; Smalley, R. E. *Appl. Phys. Lett.* **2000**, *77*, 666–668.
- (8) Choi, S. U.; Zhang, Z. G.; Yu, W.; Lockwood, F. E.; Grulke, E. A. *Appl. Phys. Lett.* **2001**, *79*, 2252–2254.
- (9) Biercuk, M. J. *Appl. Phys. Lett.* **2002**, *80*, 2767–2769.
- (10) Huxtable, S. T.; Cahuk, D. G.; Shenogin, S.; Xue, L.; Ozisik, R.; Barone, P.; Usery, M.; Strano, M. S.; Siddons, G.; Shim, M.; Keblinski, P. *Nature Mater.* **2003**, *2*, 731–734.
- (11) Frankland, S. J. V.; Caglar, A.; Brenner, D. W.; Griebel, M. J. *Phys. Chem. B* **2002**, *106*, 3046–3048.
- (12) Brenner, D. W.; Shenderova, O. A.; Areshkin, D. A.; Schall, J. D. *Comput. Model. Eng. Sci.* **2002**, *3*, 643–674.
- (13) Müller-Plathe, F. *J. Chem. Phys.* **1997**, *106*, 6082–6085.
- (14) Brenner, D. W.; Shenderova, O. A.; Harrison, J. A.; Stuart, S. J.; Ni, B.; Sinnott, S. B. *J. Phys. C* **2002**, *14*, 783–802.
- (15) Futrelle, R. P.; McGinty, D. J. *Chem. Phys. Lett.* **1971**, *12*, 285–287.

NL049645D